PHYSICAL REVIEW B VOLUME 56, NUMBER 8 15 AUGUST 1997-II

Electron transport and emission properties of C(100)

J. E. Yater, A. Shih, and R. Abrams
Naval Research Laboratory, Washington, D.C. 20375
(Received 30 May 1997)

Secondary-electron-emission spectroscopy is used to probe the transport and emission of impact-ionized electrons in single-crystal diamond. By studying the emission from a cesiated C(100) surface having a negative electron affinity (NEA), the full energy spectrum of the internal electrons is revealed in the measured energy distribution data. The kinetic energy of the electrons and the height of the surface energy barrier are measured relative to the conduction-band minimum E_c, which is identified in the spectra. The cesiated diamond surface is observed to be NEA, but the hydrogenated diamond surface (commonly believed to be NEA) has an electron affinity near zero and slightly positive. Analysis of the very high yield data ($\delta_{\max} \sim 132$) and the sharply peaked energy distribution data indicates that the transport of low-energy electrons is very efficient in C(100). An emission model is deduced that involves the surface properties of the material and the internal energy distribution of the electrons. [S0163-1829(97)50336-5]

New classes of materials have been developed recently with the promise of improved or novel electronic properties.[1–3] While electron device structures are being designed to exploit these materials,[4–7] in many cases the electronic properties of the material are not well understood. In order to develop a model that describes observed electrical behavior and predicts potential device capabilities, the electron-transport properties of the material must be investigated. In this paper, secondary-electron-emission spectroscopy is used to probe the internal energy distribution of impact-ionized electrons in a wide band gap material. Information is deduced from the data about the scattering mechanisms that govern the transport of hot electrons in the material. The position of the conduction-band minimum E_c is identified in the measured spectra, thereby providing a reference point for determining the kinetic energy of the internal electrons as well as the height of the energy barrier encountered at the surface.

Secondary-electron-emission measurements are affected by three distinct processes: electron generation in the material (using an incident electron beam), electron transport to the surface, and electron emission into vacuum. By using appropriate experimental conditions, secondary-electron-emission studies can examine the role of a particular mechanism in the secondary-emission process. In this paper, we focus on the transport of secondary electrons in a diamond sample. The C(100) surface is cesiated to produce a large negative electron affinity (NEA), thereby removing the energy barrier that usually hinders electron emission. In such a case, the emitted electron energy distribution is simply the full energy spectrum of the internal electrons that reach the surface. This energy distribution will reflect two fundamental properties of the material: (1) the density of available states in the conduction band, and (2) the scattering and recombination mechanisms which determine the energy and intensity losses suffered during transport to the surface. Thus, the energy distribution measurements can provide information about the energy states populated by impact ionization and can track the evolution of the energy distribution as the transport distance is varied.

In order to determine the electron affinity χ at the surface, the emission-onset energy must be measured relative to E_c. Without the ability to identify E_c in the energy spectra, an accurate interpretation of the electron-emission data is difficult. For example, previous electron-emission studies[8–10] of wide band gap material have interpreted the presence of a sharp peak in the energy distribution measurements as evidence of a NEA surface, although χ was not actually determined. In this paper, we obtain direct evidence of emission from a NEA surface. In contrast with earlier reports, we find that sharply peaked energy distributions do not necessarily indicate a NEA surface. The internal energy distribution of the carriers must be considered as well as the surface properties in order to accurately interpret the secondary-electron-emission data.

The sample used in this study was a $5.0 \times 5.0 \times 0.25$ mm^3 (100) p-type semiconducting diamond (natural type $2B$) from Harris Diamond corporation that was clear and transparent in appearance. The as-received diamond was mounted on a tantalum foil sample holder designed to allow resistive heating and thermocouple temperature measurement. The experiments were performed in a UHV system having a base pressure below 1×10^{-10} Torr, and measurements were taken from hydrogenated, cesiated, and bare diamond surfaces. The hydrogenation and cesiation procedures involved exposure to atomic H produced by a hot filament and evaporation from a cesium dispenser, respectively. The sample was cleaned prior to the initial hydrogenation and cesiation procedures by a thermal desorption procedure. The secondary electron yield and the energy distribution of the emitted electrons were measured for each of the three surfaces using experimental techniques that have been described in detail elsewhere.[11,12] The secondary electrons are defined to include all emitted electrons, with energy up to the incident-beam energy E_b, produced by the incident electron beam. Therefore, the secondary electron yield coefficient δ is defined as the ratio of the total emitted electron intensity to the incident electron intensity. The data are presented as secondary electron yield curves where δ is plotted as a function of E_b between 0 and 2900 eV. The energy distribution of the

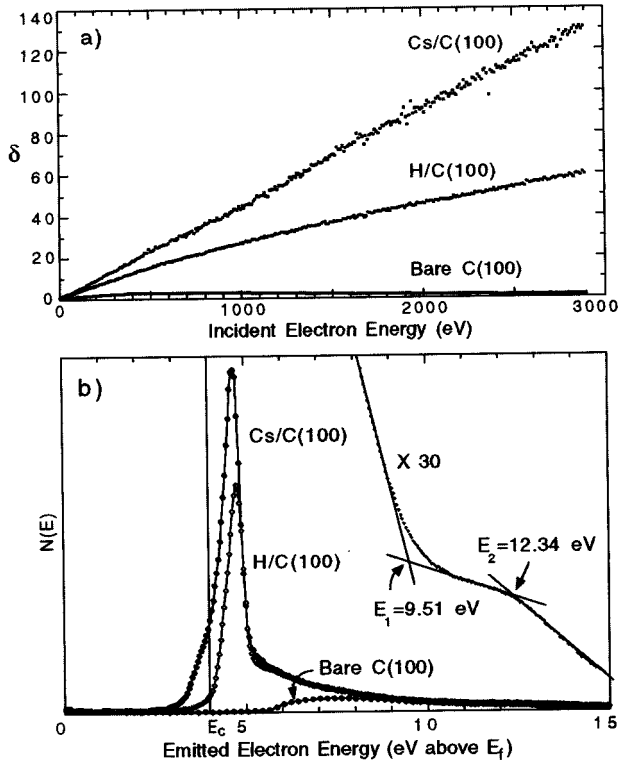

FIG. 1. Secondary-electron-emission data measured from cesiated, hydrogenated, and bare C(100) surfaces: (a) secondary electron yield curves for $E_b = 0-2900$ eV and (b) energy distribution curves taken at $E_b = 120$ eV. The offset data in (b) are magnified by a factor of 30 to illustrate the determination of the threshold energies $E_1 = E_c + E_g$ and $E_2 = E_c + \frac{3}{2}E_g$. The vertical line indicates the position of E_c deduced from the analysis of the low-energy shoulder and the thresholds at E_1 and E_2.

emitted secondary electrons was measured for each type of surface for several values of E_b using a four-grid low-energy electron diffraction (LEED) apparatus with an instrumental resolution of ~0.15 eV. Using this technique, the angle-integrated intensity is measured at each energy and the data are not convoluted by an analyzer transmission function. An energy distribution curve (EDC) is obtained by plotting the emitted electron intensity as a function of the emitted electron energy relative to the sample Fermi level E_F, where E_F is determined from the position of the σ peak of a polycrystalline graphite sample as described by Oelhafen and Freeouf.[13]

Secondary electron yield curves and EDC's measured from C(100) surfaces are shown in Figs. 1(a) and 1(b), respectively. As seen in the data, the secondary emission is tremendously enhanced by the presence of H and Cs on the surface. Specifically, the maximum yield increases from 3 for the bare surface to 60 and 132 for the hydrogenated and cesiated surfaces, respectively. It should be noted that a broad shoulder is observed at energies $E < E_c$ (where the identification of E_c is described below) from the cesiated C(100) surface but not from the hydrogenated C(100) surface. While the observation of emission energies below E_c is discussed below, the data give direct evidence of a cesiated NEA C(100) surface. However, in order to fully interpret the secondary-emission data and extract information about the

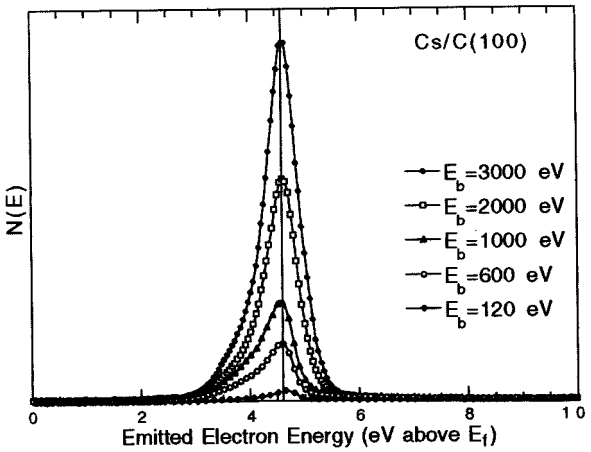

FIG. 2. EDC's measured from the cesiated C(100) sample at different incident-beam energies. The vertical line indicates the average peak position of the EDC's.

material's electronic properties, the effects of the electron generation, transport, and emission processes must be examined. The generation of electrons is controlled primarily through the parameter E_b, which can be understood by considering the electron interactions in the material. In wide band gap material, the dominant electron energy-loss mechanism is impact ionization whereby valence electrons are excited into the conduction band.[14] Throughout the paper, these injected electrons will be referred to as ''impact-ionized'' electrons. In the ionization process, the incident electron loses an amount of energy $\Delta E \geq E_g$, where the energy gap $E_g = 5.47$ eV for diamond. The exact value of ΔE depends on the scattering process and the final energy states populated by the carriers. As the incident electron energy increases, the number of possible impact-ionization events increases and the number of impact-ionized electrons thereby increases. This can be seen clearly in Fig. 1(a) where the measured yield from the cesiated C(100) surface grows linearly with E_b, and in Fig. 2 where the emission intensity increases with E_b.

In addition to the impact-ionized electrons, high-energy incident and secondary electrons are present in the material and lose energy through multiple-scattering interactions during transport to the surface. Consequently, the internal energy distribution profile has two distinct contributions: the sharp peak associated with the impact-ionized electrons and a broad energy continuum associated with higher-energy electrons. As seen in Fig. 1(b), the energy distribution of the impact-ionized electrons is centered ~0.65 eV above E_c and is quite narrow [full width at half maximum (FWHM) ~0.65–0.75 eV]. The broad, high-energy tail represents the contribution from the continuum of secondary electrons and it becomes proportionally smaller as the peak intensity increases with E_b. In fact, as E_b increases, the additional secondary electrons appear to contribute mainly to the impact-ionized peak. In the EDC's measured from the cesiated C(100) surface, the percentage of emitted electrons lying within the impact-ionized peak increases from ~60% to >96% over the range $E_b = 120-3000$ eV, as seen in Fig. 2.

The data cannot be analyzed solely on the basis of electron generation, described above, since the generated elec-

trons must travel through the material before being emitted. Hence, the electron-transport process also affects the EDC's. In particular, the penetration depth of the incident electron increases with increasing E_b, causing the secondary electrons to be generated deeper in the material. As a result, the distance the secondary electron must travel to reach the surface increases with increasing E_b, along with a greater opportunity for inelastic scattering and electron-hole recombination. For impact-ionized electrons with insufficient energy to scatter from valence electrons, the available scattering mechanisms are phonon, defect, impurity, and (if present) conduction-electron scattering. As a result, the energy distribution of the electrons reaching the surface should shift towards lower energies as the penetration depth increases, and the intensity should decrease once the rate of recombination exceeds the rate of electron generation. In the EDC's (shown in Fig. 2) taken from the cesiated diamond sample, the energy position of the impact-ionized peak does not shift as E_b is varied from 120 to 3000 eV, while the peak intensity continues to increase. This indicates that the most probable energy of the impact-ionized electrons remains essentially unchanged as the escape depth increases. In addition, it appears that the fraction of electrons captured in the material does not change appreciably as the effective transport distance increases (with increasing E_b); the ratio of measured yield δ to average internal yield $\delta_{\text{int}}=E_b/\overline{\Delta E}$ remains constant over the energy range $E_b=0-2900$ eV since both δ and δ_{int} increase linearly with E_b. Therefore, based on the yield and EDC measurements, it can be concluded that the electron-transport process for low-energy impact-ionized electrons is very efficient in the C(100) sample. While the energy distribution of the impact-ionized electrons is centered near the bottom of the conduction band, the electron-hole recombination time in the diamond is long enough to permit the transport of these electrons to the surface, at least for the range of transport distances attainable in this study.

If a surface barrier is present which blocks the emission of electrons, the energy distribution of emitted electrons will not represent the internal electron energy distribution reaching the surface. Therefore, the effect of the surface barrier height on the EDC was studied as χ was changed from negative to positive. Using the onset of emission to indicate the position of the vacuum level E_{vac}, χ was measured to be -0.90 ± 0.23 eV at the cesiated C(100) surface, in good agreement with the calculated value of -0.85 eV reported by Pickett for Cs on oxygenated C(100).[15,16] The cesiated NEA sample was heated to 300, 500, 700, 800, and 900 °C to gradually desorb the cesium and thus increase χ. In fact, χ was measured (±0.23 eV) to be -0.53, $+0.09$, $+0.15$, $+0.22$, and $+0.50$ eV after the respective heatings. Upon further heating, χ increased to $+150\pm0.23$ eV at the bare C(100) surface. This is seen in the EDC's in Fig. 3 taken at $E_b=120$ eV where, as the temperature increases, the emission threshold moves higher in energy and the impact-ionized peak decreases in intensity. While the center of the peak shifts to higher energy, the falling edge of the peak does not shift.

These observations can be understood by considering the emission model shown in Fig. 4. Because the energy distribution of the impact-ionized electrons is sharply peaked ~0.65 eV above E_c, enhanced emission will be observed as

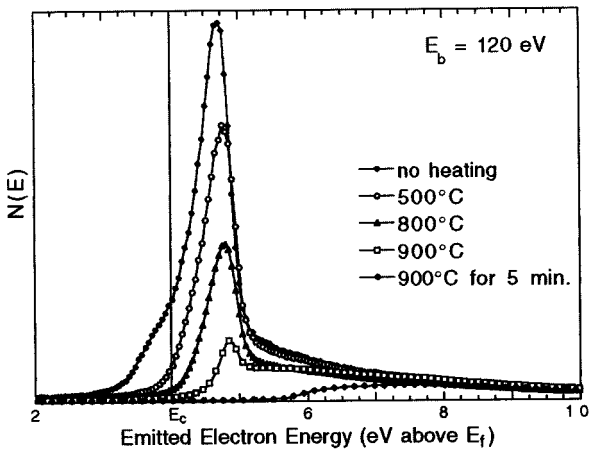

FIG. 3. EDC's measured from the cesiated C(100) sample at $E_b=120$ eV before and after sample heating. To avoid overlapping curves, the EDC's measured after the 300 and 700 °C heatings are not shown.

long as E_{vac} lies within or below this distribution. As χ increases and greater numbers of impact-ionized electrons are blocked from emission, the impact-ionized peak becomes narrower and the peak intensity decreases. It is therefore possible that a surface may have a small, positive χ and still produce sharply peaked energy distributions, as in the case of the hydrogenated C(100) surface at which $\chi=+0.12\pm0.23$ eV. Once E_{vac} rises above the peak energy, emission of the low-energy electrons is completely blocked and the peak is no longer observed in the EDC. From this emission model, it is clear that the sharp peak reflects the density of states available to the impact-ionized electrons. The peak measured from the unheated cesiated C(100) surface is nearly symmetrical in shape and relatively broad compared to the asymmetric, narrow energy distribution associated with thermalized electrons (kT=0.025 eV). The measured peak becomes increasingly narrow and asymmetric in shape as χ increases, but only because the emission of low-energy electrons is increasingly blocked. Therefore, although the internal distribution of impact-ionized electrons is not influenced by the surface/vacuum interface, the ability to probe the internal energy distribution of hot carriers is strongly affected by the surface conditions.

As stated earlier, the position of E_c must be identified in order to reference the measured features to the energy levels

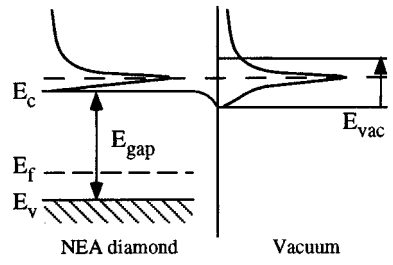

FIG. 4. Emission model for a NEA wide band gap material. The energy distribution of the emitted electrons is a convolution of the internal electron energy distribution and the electronic structure at the surface.

in the material. In this paper, certain features in the EDC's were related to E_c through a consideration of the electron scattering and emission mechanisms in the material. As discussed earlier, the ionization of valence electrons is possible only if the impacting electron energy E is above a threshold energy $E_{\min}$. For electrons with $E<E_{\min}$, the creation of electron-hole pairs is forbidden, resulting in a slower energy-loss rate and an increased emission probability. In the case of phonon-assisted scattering, the threshold energy is $E_{\min}=E_c+E_g\equiv E_1$ from energy conservation, and it represents the absolute threshold energy below which electron-hole pair creation cannot occur. If the electron scattering does not involve phonons, energy and momentum conservation dictates that $E_{\min}=E_c+\frac{3}{2}E_g\equiv E_2$,[14] although this threshold has been observed experimentally to be less stringent. While the threshold at E_1 has been described by Himpsel *et al.*[17] and was used in the analysis of data reported by Shih *et al.*,[18] the threshold at E_2 has not been previously discussed in the analysis of EDC's. We observe both excitation thresholds in our data, as indicated by the intensity changes seen in the enlarged EDC segment in Fig. 1(b), where the threshold energies E_1 and E_2 are determined by the interception of the straight lines superimposed on the data. Furthermore, the thresholds are observed at the same energies in every EDC, regardless of the surface conditions. The two energy positions are separated by 2.83 eV, which agrees well with the theoretical value $(E_2-E_1)=\frac{1}{2}E_g$. From the definitions of E_1 and E_2, the position of E_c is deduced to be 4.04 ± 0.16 and 4.13 ± 0.16 eV above E_F, respectively, for this C(100) sample.

The determination of E_c is further supported by the analysis of a broad, low-energy shoulder observed on the impact-ionized peak in EDC's measured from the cesiated C(100) surface, but not the hydrogenated C(100) surface, as seen in Fig. 1(b). However, as χ becomes positive (in Fig. 3), the shoulder disappears. The low-energy shoulder extends up to $\sim$4 eV, at which point the slope changes and the emission increases more rapidly. This can be understood by considering the emission process at a NEA surface. If the electron affinity is strongly negative, low-energy electrons at the surface which fall into energy levels below E_c can still be emitted into vacuum. The intensity of the electron emission at $E<E_c$ is limited by the specific mechanism involved in creating these electrons (i.e., inelastic scattering at the surface/vacuum interface, transitions to low-energy surface states produced by downward band bending) and the availability of the energy states. Using this model to interpret the data, the position of E_c is found to be 4.00 ± 0.16 eV above E_F. Therefore, the independent evaluations of the three separate intensity features observed in EDC's from cesiated C(100) produce the same value of E_c, within the margin of experimental error.

In summary, we used secondary-electron-emission spectroscopy to probe the transport and emission of impact-ionized electrons in a cesiated C(100) sample. Very high secondary yields were measured ($\delta_{\max}\sim132$), and the energy distribution of the emitted electrons was sharply peaked at $\sim$0.65 eV above E_c with a FWHM$\sim$0.65–0.75 eV. The data provided direct evidence of emission from a NEA surface and revealed that inelastic scattering occurs at the cesiated C(100) surface. The energy distribution and emission intensity measurements appeared relatively insensitive to the generation depth of the electrons (up to 3000 eV), indicating that the transport of low-energy secondary electrons is very efficient in the C(100) sample. In particular, the long electron-hole recombination time observed in C(100) suggests that other indirect, wide band gap materials may exhibit promising electron-transport characteristics. By studying the role of the surface barrier in the emission process, an emission model was deduced for wide band gap material that relates the observed energy spectra to the surface properties of the material and the internal energy distribution of the carriers.

The authors wish to thank Charles Hor and Lex Malsawma for their technical support. One of the authors (J.E.Y.) wishes to thank Dr. D. Scott Katzer for many helpful discussions. This work was supported by ONR and NSWC/Crane Division.

[1] S. Strite and H. Morkoc, J. Vac. Sci. Technol. B **10**, 1237 (1992).
[2] R. F. Davis, J. Cryst. Growth **137**, 161 (1994).
[3] C. Bandis and B. B. Pate, Surf. Sci. **350**, 315 (1996).
[4] M. W. Geis, J. C. Twichell, and T. M. Lyszczarz, J. Vac. Sci. Technol. B **14**, 2060 (1996).
[5] S. N. Mohammad, A. A. Salvador, and H. Morkoc, Proc. IEEE **83**, 1312 (1995).
[6] R. W. Pryor, Appl. Phys. Lett. **68**, 1802 (1996).
[7] S. C. Binari *et al.*, Solid-State Electron. **41**, 177 (1997).
[8] I. L. Krainsky, V. M. Asnin, G. T. Mearini, and J. A. Dayton, Jr., Phys. Rev. B **53**, 7650 (1996).
[9] R. E. Thomas *et al.*, in *Diamond for Electronic Applications*, edited by D. Dreifus, A. Collins, C. Beetz, T. Humphreys, K. Das, and P. Pehrsson, MRS Symposia Proceedings No. 416 (Materials Research Society, Pittsburgh, PA, 1996), p. 263.
[10] J. van der Weide *et al.*, Phys. Rev. B **50**, 5803 (1994).
[11] A. Shih and C. Hor, IEEE Trans. Electron Devices **40**, 824 (1993).
[12] A. Shih, J. Yater, C. Hor, and R. Abrams, IEEE Trans. Electron Devices **41**, 2448 (1994).
[13] P. Oelhafen and J. L. Freeouf, J. Vac. Sci. Technol. A **1**, 96 (1983).
[14] R. C. Alig and S. Bloom, Phys. Rev. Lett. **35**, 1522 (1975).
[15] W. E. Pickett, Phys. Rev. Lett. **73**, 1664 (1994).
[16] O. M. Kuttel *et al.*, Diam. Relat. Mater. **5**, 807 (1996).
[17] F. J. Himpsel, J. A. Knapp, J. A. Van Vechten, and D. E. Eastman, Phys. Rev. B **20**, 624 (1979).
[18] A. Shih, J. Yater, C. Hor, and R. Abrams, Appl. Surf. Sci. **111**, 251 (1997).